BIOCHEMISTRY

 Volume 46, Number 42 October 23, 2007

Articles

Sequence Recognition in the Minor Groove of DNA by Covalently Linked Formamido Imidazole−Pyrrole−Imidazole Polyamides: Effect of H-Pin Linkage and Linker Length on Selectivity and Affinity†

C. Caroline O'Hare,‡ Peter Uthe,§ Hilary Mackay,|| Kevin Blackmon,§ Justin Jones,§ Toni Brown,|| Binh Nguyen,⊥ W. David Wilson,⊥ Moses Lee,§,|| and John A. Hartley*,‡

Cancer Research UK Drug-DNA Interactions Research Group, Department of Oncology, University College London, 91 Riding House Street, London W1W 7BS, United Kingdom, Department of Chemistry, Furman University, Greenville, South Carolina 29613, Division of Natural and Applied Sciences and Department of Chemistry, Hope College, Holland, Michigan 49423, and Department of Chemistry, Georgia State University, Atlanta, Georgia 30303

Received May 30, 2007; Revised Manuscript Received August 7, 2007

ABSTRACT: The polyamide *N*-formamido imidazole−pyrrole−imidazole (f-ImPyIm) binds with an exceptionally high affinity for its cognate site 5′-ACGCGT-3′ as a stacked, staggered, and noncovalent cooperative dimer. Investigations are presented into its sequence specificity and binding affinity when linked covalently as an H-pin "dimer". Five f-ImPyIm cross-linked analogues with six to nine methylene linkers and an eight-linked ethylene glycol linker were examined to investigate the effect of linkage and linker length on DNA binding. Thermal denaturation studies on short DNA hairpins showed preferential binding by both f-ImPyIm ($\Delta T_m = 7.8$ °C) and its cross-linked derivatives ($\Delta T_m > 30$ °C) at 5′-ACGCGT-3′, indicating sequence specificity was retained on linkage. DNase I footprinting confirmed strict cognate site selectivity and demonstrated that affinity increased with linker length (f-ImPyIm-9 = f-ImPyIm-8 = f-ImPyIm-EG-8 > f-ImPyIm-7 > f-ImPyIm-6). The eight- and nine-linked derivatives bound at 100-fold lower concentrations at the cognate site relative to f-ImPyIm-6, and with 10-fold higher affinity than unlinked f-ImPyIm. Use of an ethylene glycol linkage in f-ImPyIm-EG-8 to improve solubility slightly increased the cognate site affinity relative to those of f-ImPyIm-8 and f-ImPyIm-9, although some selectivity was lost at high ligand concentration. CD demonstrated that cognate site binding by eight and nine-linked compounds occurred in the minor groove. SPR analysis gave a binding affinity (K) for f-ImPyIm-EG-8 at the cognate site of 2×10^{10} M^{-1}, representing a 100-fold increase relative to that of f-ImPyIm. This study demonstrates that the high-affinity cooperative binding of f-ImPyIm can be enhanced significantly by suitable covalent linkage, while maintaining its strict cognate site selectivity.

In recent years numerous structural derivatives of the DNA minor groove binding molecule distamycin A have been synthesized in an effort to exploit its highly selective DNA binding properties. Modification of the inherent specificity of distamycin A for AT base pairs to introduce a GC recognition element has been achieved by replacing some of its constituent guanine-excluding pyrrole rings with imidazoles, producing ligands able to bind selectively to DNA sequences with mixed base pair content (*1*, *2*). These oligopeptides can stack side-by-side in an antiparallel orientation within the minor groove with each peptide contacting the adjacent strand of DNA (*3*). This noncovalent cooperative binding of two unlinked polyamides forming a

† J.A.H. acknowledges program grant support from Cancer Research UK (C2259/A3083). M.L. and W.D.W. thank the NSF (Grant CHE-0550992) for support of this project.

* To whom correspondence should be addressed. E-mail: john.hartley@ucl.ac.uk. Phone: +44 (0)20 7679 9299. Fax: +44 (0)20 7436 2956.

‡ University College London.

§ Furman University.

|| Hope College.

⊥ Georgia State University.

10.1021/bi701053a CCC: $37.00
Published on Web 10/02/2007

2:1 complex with DNA enables the reading of structural information along both strands of the DNA duplex simultaneously. Each peptide's constituent heterocycles contacts a single base such that a pyrrole (Py) placed opposite a pyrrole in the corresponding ligand will bind AT or TA base pairs, an imidazole (Im) opposite a pyrrole will favor GC over CG base pairs, and an imidazole−imidazole pairing will bind either GC or CG base pairs (*4*−*6*).

Numerous footprinting and structural studies have established a set of pairing rules defining the optimal heterocycle pairs required for DNA sequence recognition at predetermined sites (*7*−*12*). These sequence-reading polyamides provide an approach to gene targeting, enabling DNA sequence discrimination with binding affinities equivalent to those of nuclear transcription factors. Such DNA binding properties offer a promising means of disrupting gene expression at predetermined sites (*13*), with recent work demonstrating the modulation of transcription of specific genes by polyamides in vitro and in cells (*14*−*25*).

Studies of the binding of unlinked N-terminal formamido triamides to their cognate sequences have demonstrated that the heterocycle combination *N*-formamido imidazole−pyrrole−imidazole (f-ImPyIm) bound with an exceptionally high affinity and selectivity for its recognition site (5′-ACGCGT-3′), relative to its parent compound distamycin A and its structural isomers for binding to their respective cognate sites (*26*, *27*). This has led to the discovery that in cooperatively bound polyamide dimers the central heterocycle pairs along the DNA strand determine the strength of binding, with a central ImPy binding the most strongly (*27*). Thus, a set of central pairing rules have been developed with the heterocycle pairs ranked −ImPy− > −PyPy− ≫ −PyIm− ≈ −ImIm− (*27*).

Although unlinked polyamides can form a 2:1 complex with DNA within the minor groove (*3*), this is not always energetically favorable (*28*). Tethering two unlinked polyamides with a suitable linker can fix the stacking arrangement of the heterocycle pairs across the groove width determining the reading frame of the DNA sequence recognized. Moreover, appropriate linkage can favor dimeric binding energetically (*29*). As the accurate alignment of the heterocycle rings alongside each base pair is crucial to providing both specificity and affinity for linked polyamides, a covalent linker must be of optimal length and geometry to position both component ligands in close proximity to the base edges within the minor groove. To achieve this, several types of structures have been used, including a hairpin motif, whereby the oligopeptides are linked head to tail using a suitable "turn peptide" (*30*) and a cross-linked H-pin structure where the central rings of two polyamide ligands are linked via a methylene bridge (*31*−*33*).

The optimal structure for DNA binding by hairpin polyamides has been investigated and reviewed (*34*); however, it is less clearly defined for H-pins. Unlike hairpin molecules, which require a three-carbon linkage or γ-turn to link two monomers "head to tail", ethidium bromide displacement, circular dichroism (CD), NMR, and molecular modeling studies have indicated that H-pin structures require a longer stretch of methylene groups to cross the groove width via the central heterocycle ring (*29*, *33*, *35*, *36*). These studies, together with more recent footprinting and gel shift data (*37*) have demonstrated that at least a five-carbon linker was

(a)

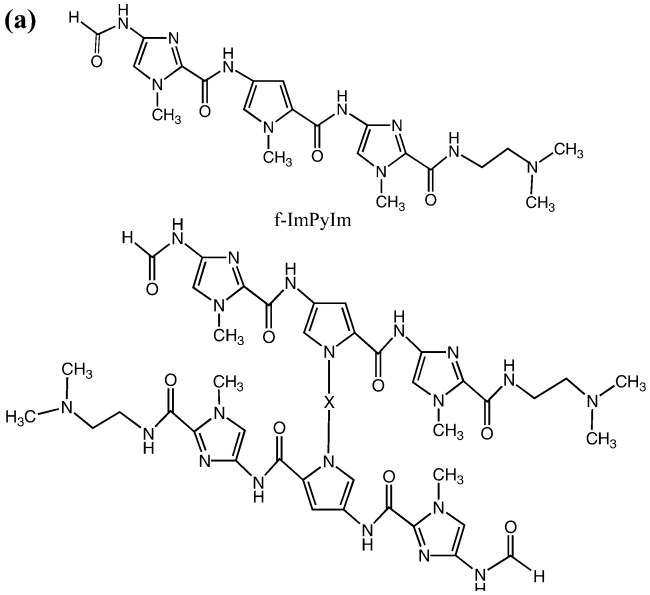

Compound	X
f-ImPyIm-6	$(CH_2)_6$
f-ImPyIm-7	$(CH_2)_7$
f-ImPyIm-8	$(CH_2)_8$
f-ImPyIm-EG-8	$(CH_2)_2O(CH_2)_2O(CH_2)_2$
f-ImPyIm-9	$(CH_2)_9$

(b)

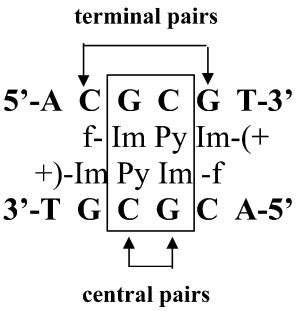

FIGURE 1: (a) Molecular structures of f-ImPyIm and its cross-linked derivatives and (b) cognate binding site for f-ImPyIm, showing the terminal and central heterocycle pairs.

required to span this distance, with linkers of seven to nine carbons providing optimal linkage depending on other structural factors such as head group and heterocycle content. A further increase in linker length has been shown to reduce both affinity and specificity, with the two polyamides slipping into a staggered motif and increasing the size of the site occupied (*29*). This observation is not surprising because most of the molecules reported do not have a formamido group at the N-terminus and they tend to stack in an overlapped fashion (*38*). In contrast, polyamides containing an N-terminus formamido group prefer to stack in a staggered fashion, thereby covering more base pairs.

Recent experiments using CD, surface plasmon resonance (SPR), isothermal titration microcalorimetry (ITC), and ^{1}H NMR have demonstrated that unlinked f-ImPyIm (Figure 1a) binds at its cognate site as a noncovalent cooperative dimer (*26*, *27*, *39*). To investigate the effect of covalent linkage on the DNA binding properties of this triamide, we present a detailed study of the in vitro DNA sequence selectivity and binding affinity of a series of cross-linked (H-pin)

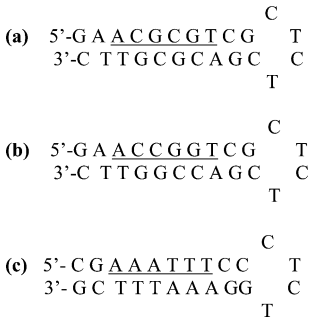

FIGURE 2: Three synthetic hairpins containing (a) the cognate site for f-ImPyIm, 5′-ACGCGT-3′, and the noncognate sites (b) 5-ACCGGT-3′ and (c) 5′-AAATTT-3′.

molecules based on this polyamide. Two f-ImPyIm triamides were linked covalently across the central heterocycle rings by a range of linkers comprised of six- to nine-atom chains as shown in Figure 1a, with the goal of binding as a cross-linked dimer in which the polyamide moieties are stacked in a staggered manner. Footprinting and biophysical studies including thermal denaturation, CD, and SPR were used to test their specificity, affinity, stoichiometry, and mode of binding at a number of DNA sequences including 5′-ACGCGT-3′, the cognate sequence for unlinked f-ImPyIm (Figure 1b).

EXPERIMENTAL PROCEDURES

Compounds. f-ImPyIm was synthesized following published procedures (*26*), and the preparation of H-pins f-ImPyIm- (*6*−*9*) and f-ImPyIm-EG-8 will be reported elsewhere.

DNA Thermal Denaturation. The synthetic DNA hairpins given in Figure 2 used in these studies were obtained from Operon (Huntsville, AL). Thermal denaturation data were obtained using a Cary Bio 100 spectrophotometer and cells with a 10 mm path length. Experiments were performed in $PO_4$0 (10 mM sodium phosphate, 1 mM EDTA, pH 6.2) with 1 μM oligonucleotide and 3 μM ligand. Oligonucleotide samples were reannealed prior to denaturation studies by being heated at 70 °C for 1 min and then allowed to cool to room temperature. The temperature was programmed to ramp from 25 to 95 °C at a rate of 0.5 °C min^{-1}, recording the absorbance at 260 nm every 0.5 °C. The data were analyzed using the KaleidaGraph (Synergy Software, Reading, PA) and the melting temperature (T_m) values determined as the maximum of the first derivative.

DNase I Footprinting. A radiolabeled DNA fragment of 125 base pairs was generated by polymerase chain reaction as follows. A 4 pmol portion of reverse primer 5′-GTCGGTTAGGAGAGCTCCACTTG-3′ (MWG Biotech) was 5′-^{32}P-end-labeled with [γ-^{32}P]ATP using T4 kinase (Invitrogen) following standard protocols. The labeled primer was then added to 4 pmol of forward primer 5′-CTGTCCAGAAAGCCGGCACTCAG-3′ (MWG Biotech), 0.125 pmol of bottom strand template oligonucleotide IM17 (5′-AAAGTCGGTTAGGAGAGCTCCACTTGCTTGAAGAGCGCTACTAGAGTTACGTGTAGATCTAGAGAAATTTCTGTGAACACCGGTGATCAAGATGACGCGTTTGTAGACTGAGTGCCGGCTTTCTGGAGCAT-3′, Eurogentec), 0.125 pmol of top strand template IM19 (5′-ATGCTCCAGAAAGCCGGCACTCAGTCTACAAACGCGTCATCTTGATCACCGGTGTTCACAGAAATTTCTCTAGATCTACACGTAACTCTAGTAGCGCTCTTCAAGCAAGTGGAGCTCTCTCCTAACCGACTTT-3′, Eurogentec), 2.5 μL of 2.5 mM dNTPs (Promega), 5 U of Taq polymerase (Promega), 2 μL of 25 mM $MgCl_2$, and 5 μL of 10× thermophilic DNA polymerase buffer (Promega) to a final volume of 50 μL, and a polymerase chain reaction was carried out as follows: 3 min at 95 °C, 1 min at 94 °C, 1 min at 63 °C, and 1 min at 72 °C for 35 cycles. The resulting labeled fragment was purified on a Bio-Gel P-6 column (Biorad) followed by agarose gel electrophoresis and isolated using a Geneclean II kit (VWR) according to the manufacturer's instructions. DNase I footprint reactions were performed by incubating polyamides with a 1000 cps 5′-single-end-labeled fragment in 10 mM Tris, pH 7.0, 1 mM EDTA, 50 mM KCl, 1 mM $MgCl_2$, 0.5 mM DTT, and 40 mM Hepes, pH 7.9, at room temperature for 30 min in a total volume of 50 μL. Cleavage by DNase I was carried out at room temperature and initiated by the addition of 2 μL (0.5 U) of DNase I diluted in ice-cold 10 mM Tris, pH 7.0, from a stock solution (1 U/μL, Promega) and 1 μL of a solution of 250 mM $MgCl_2$ and $CaCl_2$. The reactions were stopped after 3 min by the addition of 100 μL of a stop mix containing 200 mM NaCl, 30 mM EDTA, pH 8, and 1% SDS. The cleavage products were precipitated in the presence of 1 μL of glycogen (20 mg/mL, Roche Diagnostics), washed once in 80% ethanol, and dried. The samples were resuspended in formamide loading buffer (95% formamide, 20 mM EDTA, 0.05% bromophenol blue, 0.05% xylene cyanol), denatured for 5 min at 90 °C, cooled on ice, and electrophoresed at 1500 V for 2 h on a 10% acrylamide denaturing gel (Sequagel, National Diagnostics). The gels were dried under vacuum at 80 °C and exposed to film for 24 h (Super RX, Fuji).

CD Titration. CD studies were performed on a JASCO J-710 spectrophotometer at ambient temperature in a 1 mm path length cuvette. The initial DNA concentration was 9 μM in $PO_4$20 (10 mM phosphate, 200 mM Na^+, 1 mM EDTA, pH 6.2), and a solution of ligand was titrated in aliquots of between 0.3 and 1 molar equiv past the point of saturation. The CD response at the λ_{max} of the induced peak was plotted against the mole ratio of ligand to DNA to determine the stoichiometry of the binding reaction.

SPR Studies. The biosensor experiments were conducted in degassed phosphate buffer (0.19 M NaCl, 10 mM sodium phosphate, 1 mM disodium EDTA, 0.00005% (v/v) 10% surfactant P20 (Biacore), pH 6.25) at 25 °C. The 5′-biotin-labeled (attached by a 12-atom linker) DNA hairpins were purchased from Integrated DNA Technologies (Coralville, IA) or Midland Certified Reagent Co. (Midland, TX) with HPLC purification. The DNA sequences are 5′-biotin-GAACGCGTC*CTCT*GACGCGTTC-3′, 5′-biotin- GAACCGGTC*CTCT*GACCGGTTC-3′, and 5′-biotin-CGAAATTTC*CTCT*GAAATTTCG-3′ (denoted as ACGCGT, ACCGGT, and AAATTT, respectively; hairpin loops are in italic font). The experiments were conducted with a Biacore 3000 instrument (Biacore AB). The DNA hairpins were immobilized on a streptavidin-derivatized dextran−gold chip (SA chip from Biacore) by manual injection of 25 nM hairpin DNA solution with a flow rate of 1 μL/min until the response units reached about 450 RUs. Flow cell 1 was left blank, while flow cells 2, 3, and 4 were immobilized with three different hairpins. Typically, a series of different concentra-

Table 1: Melting Temperatures (T_m, °C) for Unlinked f-ImPyIm, the Linked H-Pin f-ImPyIm Compounds, and Distamycin

polyamide (PA)	T_M, T_M(+PA), ΔT_m (°C)		
	ACGCGT	ACCGGT	AAATTT
f-ImPyIm	71.2, 79.0, 7.8	69.8, 70.9, 1.1	54.9, 55.8, 0.9
f-ImPyIm-6	71.2, >95, >30	69.8, 75.3, 5.5	54.9, 64.5, 9.6
f-ImPyIm-7	71.2, >95, >30	69.8, 73.3, 3.5	54.9, 66.0, 11.1
f-ImPyIm-8	71.2, >95, >30	69.8, 76.4, 6.6	54.9, 63.2, 8.3
f-ImPyIm-EG-8	71.2, >95, >30	69.8, 83.9, 14.1	54.9, 64.2, 9.3
f-ImPyIm-9	71.2, >95, >30	69.8, 78.8, 9.0	54.9, 60.9, 6.0
distamycin A	71.2, 0.0, 0.0	69.8, 71.8, 2.0	54.9, 68.7, 13.8

tions of ligand were injected onto the chip with a flow rate of 100 μL/min for a period of 2.5 min followed by a dissociation period of 20 min. After every cycle the chip surface was regenerated with a 30 s injection of 400 mM NaCl, 20 mM NaOH solution and multiple 1 min buffer injections. The data were processed with BIAevaluation software (*40*) by kinetic fittings.

Computer-Generated Depiction. The 3D depiction of the f-ImPyIm-EG-8/5′-CCACGCGTGG-3′ complex was generated using SYBYL 7.0 on a Silicon Graphics workstation. B-form double helical DNA was generated in SYBYL, and the complex was constructed using the published unlinked f-ImPyIm/CGCG complex (*39*) by building the ethylene glycol linker joining the two polyamide moieties through the central pyrrole group at N1. The complex in water, without ions, was then structurally optimized in a 1000-step minimization using the SYBYL force field.

RESULTS AND DISCUSSION

Chemistry. The methylene-linked triamides had problems with solubility and tended to form aggregates at the concentrations required for some of the biophysical analysis, including SPR. This led to an effort to improve H-pin solubility by altering the structure of the linker. Two of the constituent CH_2 moieties were replaced with O atoms in the linker, producing an ethylene glycol H-pin composed of a chain of eight atoms. The result was the production of a more water-soluble compound, f-ImPyIm-EG-8, over its alkyl-linked counterparts.

Thermal Denaturation Studies. The sequence specificity of the linked H-pin f-ImPyIm series was tested using three DNA hairpins (Figure 2) in thermal denaturation experiments. The DNA hairpins examined contained the following sequences: 5′-ACGCGT-3′, shown in previous studies to be the cognate binding site for unlinked f-ImPyIm (*26*), 5′-ACCGGT-3′, an alternative GC-rich site, and 5′-AAATTT-3′, the cognate site for distamycin A. Thermal denaturation experiments screened the preferred binding sequences of the five linked f-ImPyIm compounds by measuring their ability to stabilize each double-stranded DNA sequence on binding. ΔT_m values were derived from the differences in melting temperature of the DNA−triamide complexes and duplex DNA alone and are shown in Table 1. ΔT_m values for unlinked f-ImPyIm and distamycin A were also included for comparison.

Unlinked f-ImPyIm gave a ΔT_m value of 7.8 °C when bound to its cognate site 5′-ACGCGT-3′. This was an 8-fold increase in melting temperature relative to that given by f-ImPyIm with 5′-ACCGGT-3′ (ΔT_m = 1.1 °C), a site differing by only two base pairs. All five linked f-ImPyIm derivatives gave an exceptional degree of stabilization recorded for the cognate hairpin (ΔT_m > 30 °C). Selectivity for the cognate site was retained on linkage, with all five H-pin-linked f-ImPyIm homologues showing a strong preference for 5′-ACGCGT-3′. However, as exact T_m values could not be obtained at the cognate site for the H-pin series due to the very high degree of stabilization, a precise measure of the selectivity of these compounds for this sequence relative to that of f-ImPyIm could not be determined. As a result, only approximate comparisons of duplex stabilization could be made between the different sites. Nevertheless, a 4-fold increase in duplex stabilization was observed at this site with the linked homologues relative to unlinked f-ImPyIm (ΔT_m = 7.8 °C). In addition, at least a 2-fold (f-ImPyIm-EG-8) and at least a 10-fold (f-ImPyIm-7) increase in melting temperature was observed at the cognate site relative to 5′-ACCGGT-3′. Duplex stabilization was also observed with the linked compounds at 5′-AAATTT-3′. This was in contrast to unlinked f-ImPyIm, which showed no stabilization of this site (ΔT_m = 0.9 °C). However, the ΔT_m values obtained for 5′-AAATTT-3′ with the linked derivatives ranged from 6.0 to 11.1 °C, which was significantly lower than those obtained for the cognate site. As expected distamycin A stabilized 5′-AAATTT-3′ (ΔT_m = 13.8 °C), its own cognate site, but showed little or no stabilization of the noncognates 5′-ACGCGT-3′ (ΔT_m = 0.0 °C) and 5′-ACCGGT-3′ (ΔT_m = 2.0 °C).

DNase I Titration Studies. DNase I footprinting was used to examine the selectivity of the H-pin-linked f-ImPyIm series for the cognate site 5′-ACGCGT-3′, the noncognate GC-rich site 5′-ACCGGT-3′, and the AT-rich site 5′-AAATTT-3′ when placed within a single DNA fragment of 131 base pairs (Figure 3). Typical footprint titrations for f-ImPyIm, f-ImPyIm-6, f-ImPyIm-7, f-ImPyIm-8, f-ImPyIm-EG-8, and f-ImPyIm-9 are shown in Figure 4. The titration result for unlinked f-ImPyIm was reported (*39*). It is included here for comparison with the linked f-ImPyIm titration results. These compounds did not appear to bind at any other sites along the DNA fragment examined, including at 5′-ACCGGT-3′, at concentrations up to the millimolar range, thereby corroborating the sequence preference observed in the thermal denaturation data. No significant binding was observed at any other sites, indicating that linkage of f-ImPyIm in this way did not compromise its strong selectivity.

Affinity for the cognate binding site, as indicated by the onset of ligand binding, increased with the linker length within the H-pin series. The eight- and nine-linked compounds produced the strongest binding at 5′-ACGCGT-3′, with a 100-fold difference in the concentrations required for binding observed between f-ImPyIm-6 (0.5 μM) and f-ImPyIm-9 (0.005 μM). Moreover, binding with f-ImPyIm-8 and f-ImPyIm-9 occurred at a 10-fold lower concentration (0.005 μM) than with f-ImPyIm (0.05 μM), indicating an increased affinity for this site relative to that of the monomer. However, linkage did not always improve binding relative to unlinked f-ImPyIm, with binding initiated at only 0.5 μM with f-ImPyIm-6 and at 0.05−0.1 μM with f-ImPyIm-7. These data are consistent with previous footprinting and gel shift analyses of H-pin-linked triamides (*37*).

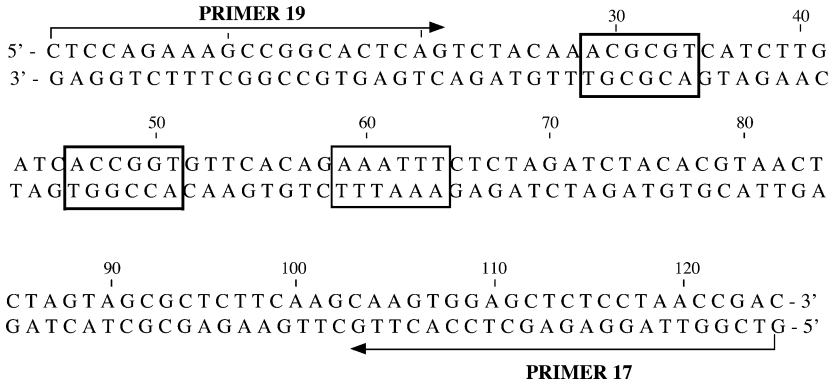

FIGURE 3: DNA fragment used for the footprint titrations. The sequences 5′-ACGCGT-3′, 5′-ACCGGT-3′, and 5′AAATTT-3′ are highlighted with black boxes. Primer sequences (19 and 17) used to generate the fragment are indicated with an arrow.

The ethylene glycol-linked molecule f-ImPyIm-EG-8, designed to improve H-pin solubility, was also selective for the cognate site. It showed a slightly increased affinity for the cognate site relative to f-ImPyIm-8 and f-ImPyIm-9, with the onset of binding occurring at 0.001−0.005 μM. A small amount of binding was also observed at the 5′-ACCGGT-3′ site, but this occurred at high concentrations of ligand, at least 100-fold higher than for binding at the cognate site.

Circular Dichroism Analysis. CD spectroscopy was used to establish the DNA groove binding mechanism of the eight- and nine-linked f-ImPyIm ligands (f-ImPyIm-8, f-ImPyIm-9, and f-ImPyIm-EG-8). CD assays were carried out by titrating each ligand with DNA solutions comprised of the three hairpins tested in the thermal denaturation studies, containing either the cognate binding site 5′-ACGCGT-3′ or the noncognates 5′-ACCGGT-3′ and 5′-AAATTT-3′ (Figure 5). As these compounds are nonchiral, they do not normally show a CD signal. However, on addition of polyamide to the cognate site, distinct CD bands were induced around 330 nm for all three of the linked polyamides examined, indicative of ligand binding in the DNA minor groove (*41*, *42*). Polyamides were titrated until no further change was observed in the CD spectra, indicating a saturation of the available DNA binding sites. Saturation was observed for f-ImPyIm-EG-8 at ∼2 mol of ligand/mol of DNA hairpin, which is indicative of nonspecific binding due to the relatively high DNA concentrations used in the experiments as previously reported (*43*). The stoichiometries for f-ImPyIm-8 and -9 were more difficult to ascertain because they had a tendency to form aggregates in aqueous solutions.

Comparison of the CD spectrum of f-ImPyIm-EG-8 with those of the three DNA hairpins (Figure 5) demonstrated that the largest signal induced at ∼330 nm at the saturating concentration occurred with the cognate site 5′-ACGCGT-3′, which is consistent with polyamides that have high binding affinity (*26*). A good response was also induced at ∼330 nm on the addition of the polyamides to 5′-ACCGGT-3′and 5′-AAATTT-3′, indicating that these molecules were attracted to the DNA minor groove. These results correlated with preferential binding of 5′-ACGCGT-3′ by these compounds as observed by thermal denaturation, footprinting, and SPR studies, which gave a high binding affinity for f-ImPyIm-EG-8 ($K = 2 \times 10^{10}$ M^{-1}) as described below.

Surface Plasmon Resonance Studies. SPR analysis of the binding of f-ImPyIm-EG-8 to the three sequences 5′-biotin-ACGCGT-3′, 5′-biotin-ACCGGT-3′, and 5′-biotin-AAATTT-3′ quantifies its binding affinity at these sites and gives a measure of the selectivity of an eight-linked f-ImPyIm H-pin for its cognate site. The SPR results also provide an indication of the stoichiometry of the binding reactions. Similar studies were attempted on f-ImPyIm-8 and -9, but were unsuccessful because the compounds have a strong propensity to form aggregates in solution and "stick" tightly to the injection tubes and flow cells on the SPR instrument. Sensorgrams obtained for the binding of f-ImPyIm-EG-8 to biotin-immobilized DNA hairpins containing the sequences 5′-ACGCGT-3′ and 5′-ACCGGT-3′ are shown in parts a and b, respectively, of Figure 6. The observed RU_{max} values are the same as the calculated value for one ligand bound, which indicates a 1:1 binding stoichiometry. For the 5′-ACGCGT-3′ hairpin, the response of the dissociation phase hardly decreases in the experimental time period, and this makes the kinetic fits unreliable. Thus, the binding constant for this complex was estimated to be 2×10^{10} M^{-1}, the largest binding constant among polyamides recorded in our laboratories. The very tight binding of f-ImPyIm-EG-8 to 5′-ACGCGT-3′ indicates at least a 200-fold increase in affinity relative to that for 5′-ACCGGT-3′ (see below), a 100-fold increase relative to that of unlinked dimer f-ImPyIm to the same sequence (1.9×10^8 M^{-1}), and a 1000-fold increase relative to that of the binding of nature's compound distamycin A to its cognate 5′-AAATTT-3′ (1.7×10^7 M^{-1}) (*26*). These values are in excellent agreement with footprint results at nanomolar concentrations.

The sensorgrams for the interaction of f-ImPyIm-EG-8 with the 5′-biotin-ACCGGT-3′ hairpin were somewhat similar to those of unlinked f-ImPyIm with 5′-ACGCGT-3′ (*26*). The results were fit with a 1:1 model with a mass transport term (*44*, *45*) as previously described (*46*). The parameters obtained from the fits are $k_a = 2.2 \times 10^5$ M^{-1} s^{-1}, $k_d = 2.0 \times 10^{-3}$ s^{-1}, and $RU_{max} = 83$, and the mass transfer coefficient k_t is 9.8×10^6 RUs M^{-1} s^{-1}. The ratio of the rate constants yielded a binding affinity of 1.1×10^8 M^{-1} for the f-ImPyIm-EG-8/ACCGGT complex. The set of sensorgrams in both association and dissociation phases is fit to the binding model by a global fit routine (*47*). Any baseline errors will have a larger fraction on the signal at the lowest concentrations. However, if the lowest concentration sensorgrams are deleted and the remaining sensorgrams are fit, the K_a value changes by less than 10%. The parameters obtained from the fit satisfy the condition where

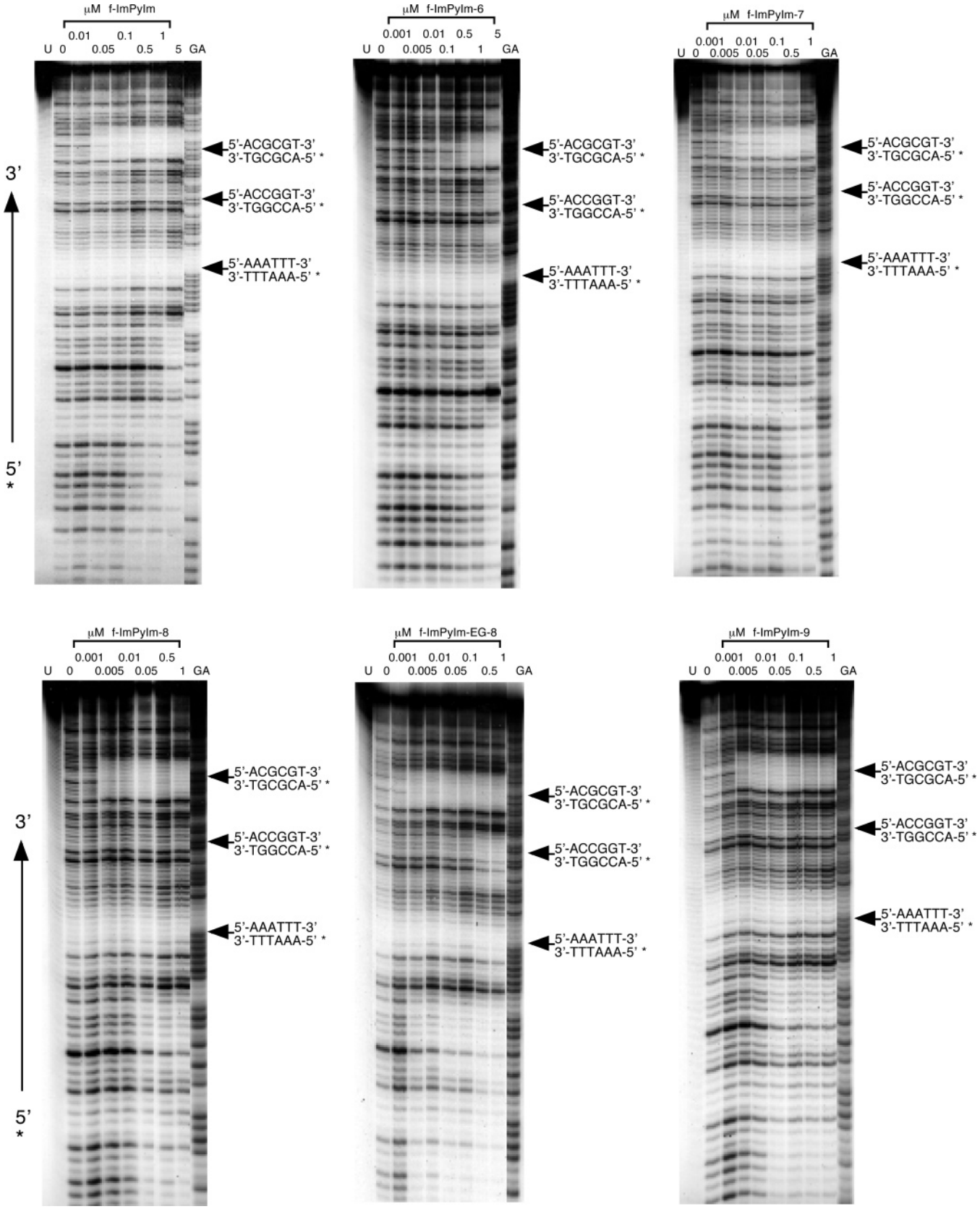

FIGURE 4: DNase I footprinting of f-ImPyIm, f-ImPyIm-6, f-ImPyIm-7, f-ImPyIm-8, f-ImPyIm-EG-8, and f-ImPyIm-9 on the antisense strand of the 5′-^{32}P-labeled 125 bp fragment showing the sites 5′-ACGCGT-3′, 5′-ACCGGT-3′, and 5′-AAATTT-3′. All reactions contain a 1000 cps DNA fragment, 10 mM Tris, pH 7, 1 mM EDTA, 50 mM KCl, 1 mM $MgCl_2$, 0.5 mM DTT, and 20 mM Hepes. "U" denotes undigested DNA and "GA" the purine sequencing lane.

the mass transfer process is minimized, $k_a(RU_{max})/k_t < 5$ (*45*); this indicates the rate constants from the fit are reliable. Relatively strong binding was observed at 5′-ACCGGT-3′ with f-ImPyIm-EG-8 ($K = 1.1 \times 10^8$ M^{-1}) although it was not the cognate site. The dissociation rate constant for this complex ($k_d = 2.0 \times 10^{-3}$ s^{-1}) was the same as that

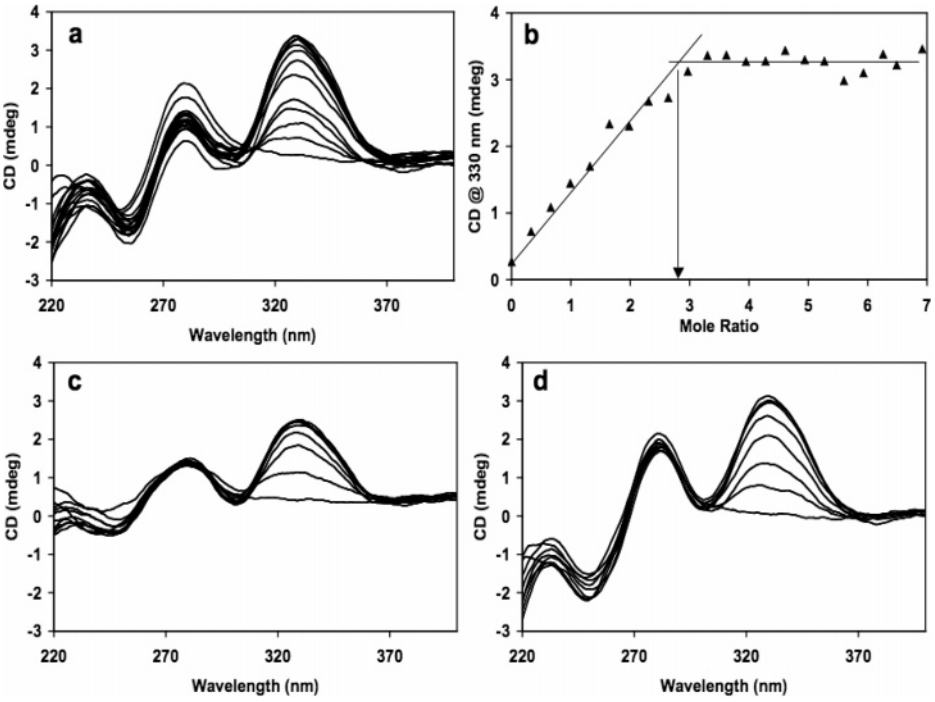

FIGURE 5: (a) CD spectra of f-ImPyIm-EG-8 binding to 5′-ACGCGT-3′. (b) CD response of the CD signal at λ_{max} (328 nm) versus the mole ratio of ligand to ACGCGT. (c, d) CD spectra of f-ImPyIm-EG-8 binding to 5′-ACCGGT-3′ and 5′-AAATTT-3′, respectively.

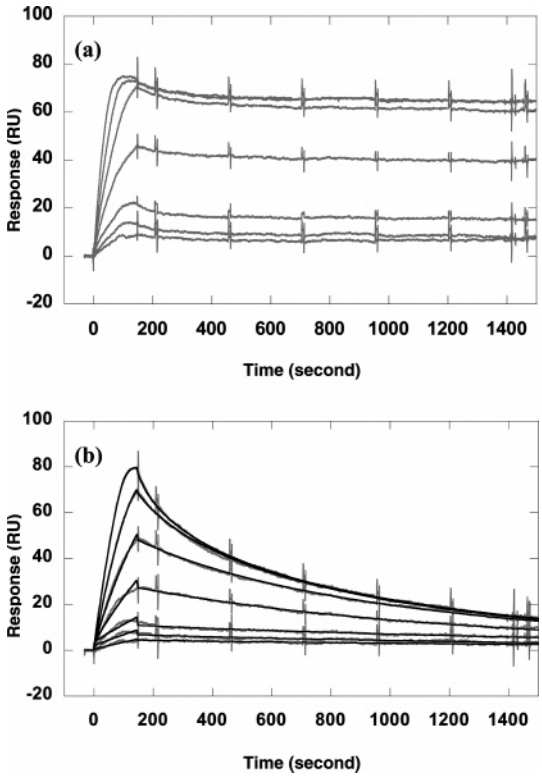

FIGURE 6: Representative SPR sensorgrams (gray) for the interaction of f-ImPyIm-EG-8 with the DNA hairpins (a) 5′-biotin-ACGCGT-3′ and (b) 5′-biotin-ACCGGT-3′. The kinetic fits (black lines) are also shown for ACCGGT. The free ligand concentrations from bottom to top are 0.008, 0.01, 0.02, 0.04, 0.06, 0.08, and 0.1 μM. The sensorgrams are shown in the same range for both hairpins for direct comparison.

calculated from the dissociation phase of the highest concentration sensorgram using the relationship $k_d = \ln(2)/t_{1/2}$, where $t_{1/2}$ is the time it takes for 50% of the complex to dissociate. The enhanced binding at this site supported the CD data, which also showed a strong response with f-ImPyIm-EG-8 at this site. Indeed, the binding affinity was similar in magnitude to that observed with f-ImPyIm for its cognate site (*26*).

Much weaker binding to the 5′-biotin-AAATTT-3′ hairpin was observed. The sensorgrams (not shown) reached a steady-state plateau even at low compound concentrations. In this case, the binding constant can be determined from steady-state fittings. The binding affinity is much weaker as expected for this A/T sequence, $K = 5 \times 10^5$ M^{-1}. This demonstrated a marked improvement in the affinity of binding at the cognate site on linkage of f-ImPyIm triamides.

Computer-Generated Depiction. On the basis of evidence that the f-ImPyIm H-pin molecules bind selectively in the minor groove of 5′-ACGCGT-3′, in a manner similar to that reported for a stacked dimer formed from unlinked f-ImPyIm (*39*), a computer-generated model of the complex of f-ImPyIm-EG-8 bound to a self-complementary duplex, 5′-CCACGCGTGG-3′, was produced and is shown in Figure 7. The model provides a graphical visualization of the complex formation. The cross-linked and stacked polyamide fits snugly within the minor groove and forms specific contacts with the floor and wall of the groove. The ethylene glycol linker provides sufficient length for the polyamides to stack in a staggered manner. Finally, the oxygen atoms in the linker point out from the complex to maximize interactions with water molecules. The interactions could contribute to the improved solubility and binding affinity of f-ImPyIm-EG-8 to 5′-ACGCGT-3′.

CONCLUSION

Recent studies demonstrate that unlinked f-ImPyIm has an exceptional binding affinity for its cognate site given its small size, binding with a 10-fold and 250-fold increased affinity relative to its parent molecule distamycin A and its structural isomer f-PyImIm, respectively, for their recognition

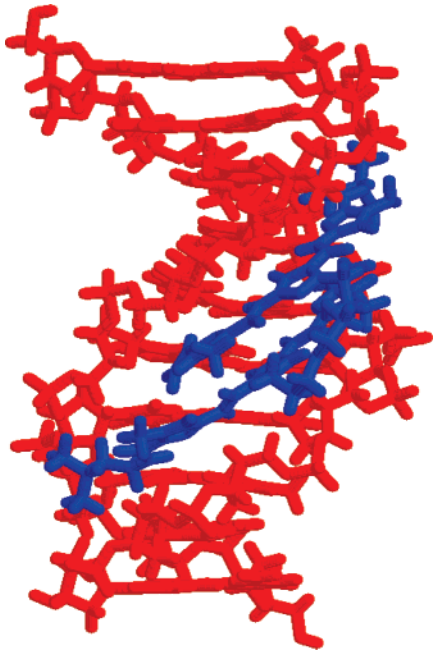

FIGURE 7: Computer-generated model of the f-ImPyIm-EG-8/5′-CCACGCGTGG-3′ complex using SYBYL 7.0.

sequences (*26*). This interaction has been shown by CD, SPR, and ^{1}H NMR to involve cooperative binding in a 2:1 ratio of ligand to DNA (*26*, *27*, *39*). Moreover, NMR and ITC data indicate that the unusually strong affinity f-ImPyIm has for its cognate site in a 2:1 complex is due to the more ordered and thermodynamically favorable structure it forms in this complex compared to that formed by its isomer f-PyImIm (*39*). The findings presented here demonstrate that appropriate covalent linkage of two f-ImPyIm ligands, in this case using either a methylene or preferably an ethylene glycol H-pin linker eight or nine atoms in length, can further increase the already exceptional affinity observed on the cooperative binding of two f-ImPyIm triamides at the cognate site. The increase in affinity may range from at least 10-fold as demonstrated by the footprinting data to 100-fold as shown by SPR. Importantly, this is not accompanied by a loss of specificity, which can often be concomitant with a gain in DNA binding affinity (*48*−*51*).

The biophysical interactions responsible for the large increase in affinity observed on covalent dimerization of f-ImPyIm relative to that of a cooperatively bound dimer are as yet unclear. Fluorescence-detected stopped-flow experiments with unlinked, hairpin, and cyclic polyamides have demonstrated that large differences in the equilibrium association constants observed between the unlinked and covalently linked molecules were primarily due to the higher association rate constants (*52*). It is possible that an appropriate covalent linkage can favor dimeric binding energetically by providing an overall binding affinity that exceeds the product of two stepwise binding constants resulting from the cooperative binding of two separate monomers (*29*).

Other thermodynamic components, such as the uptake and release of water molecules from the polyamide/DNA complex or salt-mediated interactions, are yet undefined. However, although the biophysical mechanism for dimeric polyamide binding is currently unclear, the value of suitable covalent linkage in this case using an eight-atom H-pin linker is unambiguous. Here it has been shown to enhance binding affinity without a loss of sequence specificity. Moreover, small modifications of the linker structure, introducing two O atoms into the linking chain, made a significant improvement in compound solubility. This demonstrates that the linker itself can be used to change the biophysical properties of the overall molecule without a detrimental effect on the DNA binding properties of the compound.

The continuing expansion of the structural rules for polyamide interactions, most recently by the elucidation of the key role of the central heterocycle pair, has resulted in improvements in polyamide design, enabling the highly selective targeting of DNA sequences. Understanding of the biophysical interactions that influence these rules, together with a greater knowledge of the mechanism of both noncovalent and covalent dimeric binding, will provide further insight into the optimization of novel polyamide structures.

ACKNOWLEDGMENT

We thank Chrystal Bruce at Erskine College for the computer-generated depiction.

REFERENCES

1. Kopka, M., L., Yoon, C., Goodsell, D. S., Pjura, P., and Dickerson, R. E. (1985) The molecular origin of DNA-drug specificity in netropsin and distamycin, *Proc. Natl. Acad. Sci. U.S.A. 82*, 1376−1380.
2. Lown, J. W., Krowicki, K., Bhat, U. G., Skorobaty, A., Ward, B., and Dabrowiak, J. C. (1986) Molecular recognition between oligopeptides and nucleic acids: novel imidazole-containing oligopeptides related to netropsin that exhibit altered DNA sequence specificity, *Biochemistry 25*, 7408−7416.
3. Pelton, J. G., and Wemmer, D. E. (1989) Structural characterisation of a 2:1 distamycin A. d(CGCGAAATTGGCC)$_2$ complex by two dimensional NMR, *Proc. Natl. Acad. Sci. U.S.A. 86*, 5723−5727.
4. Wade, W. S., Mrksich, M., and Dervan, P. B. (1992) Design of peptides that bind in the minor groove of DNA at 5′-(A,T)G-(A,T)C(A,T)-3′ sequences by a dimeric side-by-side motif, *J. Am. Chem. Soc. 114*, 8783−8794.
5. Mrksich, M., Wade, W. S., Dwyer, T. W., Geierstanger, B. H., Wemmer, D. E., and Dervan, P. B. (1992) Antiparallel side-by-side dimeric motif for sequence specific recognition in the minor groove of DNA by the designed peptide 1-methylimidazole-2-carboxamide netropsin, *Proc. Natl. Acad. Sci. U.S.A. 89*, 7586−7590.
6. Wade, W. S., Mrksich, M., and Dervan, P. B. (1993) Binding affinities of synthetic peptides, pyridine-2-carboxamidenetropsin and 1-methylimidazole-2-carboxamidenetropsin, that form 2:1 complexes in the minor groove of double stranded helical DNA, *Biochemistry 32*, 11385−11389.
7. Mrksich, M., and Dervan, P. B. (1993) Antiparallel side-by-side heterodimer for sequence specific recognition in the minor groove of DNA by a distamycin/1-methylimidazole-2-carboxamide-netropsin pair, *J. Am. Chem. Soc. 115*, 2572−2576.
8. Geierstanger, B. H., Jacobsen, J. P., Mrksich, M., Dervan, P. B., and Wemmer, D. E. (1994) Structural and dynamic characterisation of the heterodimeric and homodimeric complexes of distamcyin and 1-methylimidazole-2-carboxamide-netropsin bound to the minor groove of DNA, *Biochemistry 33*, 3055−3062.
9. Geierstanger, B. H., Mrksich. M., Dervan, P. B., and Wemmer, D. E. (1994) Design of a GC specific DNA minor groove-binding peptide, *Science 266*, 646−650.
10. Mrksich, M., and Dervan, P. B. (1995) Recognition in the minor groove of DNA at 5′-(A,T)GCGC(A,T)-3′ by a four ring tetrapeptide dimer. Reversal of the specificity of the natural product distamycin, *J. Am. Chem. Soc. 117*, 3325.
11. Kielkopf, C. L., Baird, E. E., Dervan, P. B., and Rees, D. C. (1998) Structural basis for GC recognition in the DNA minor groove, *Nat. Struct. Biol. 5*, 104−109.

12. Kielkopf, C. L., White, S., Szewczyk, J. M., Turner, J. M., Baird, E. E., Dervan, P. B., and Rees, D. C. (1998) A structural basis for recognition of A. T and T. A base pairs in the minor groove of B-DNA, *Science 282*, 111−115.
13. Trauger, J. W., Baird. E. E., and Dervan, P. B. (1996) Recognition of DNA by designed ligands at subnanomolar concentrations, *Nature 382*, 559−561.
14. Gottesfeld, J. M., Neely, L., Trauger, J. W., Baird, E. E., and Dervan, P. B. (1997) Regulation of gene expression by small molecules, *Nature 387*, 202−205.
15. Dickinson, L. A., Gulizia, R. J., Trauger, J. W., Baird, E. E., Mosier, D. E., Gottesfeld, J. M., and Dervan, P. B. (1998) Inhibition of RNA polymerase II transcription in human cells by synthetic DNA-binding ligands, *Proc. Natl. Acad. Sci. U.S.A. 95*, 12890−12895.
16. Dickinson, L. A., Trauger, J. W., Baird, E. E., Ghazal, P., Dervan, P. B., and Gottesfeld, J. M. (1999) Anti-repression of RNA polymerase II transcription by pyrrole-imidazole polyamides, *Biochemistry 38*, 10801−10807.
17. Dickinson, L. A., Trauger, J. W., Baird, E. E., Dervan, P. B., Graves, B. J., and Gottesfeld, J. M. (1999) Inhibition of ets-1 DNA binding and ternary complex formation between ets-1, NF-κb and DNA by a designed DNA-binding ligand, *J. Biol. Chem. 274*, 12765−12773.
18. Mapp, A. K., Ansari, A. Z., Ptashne, M., and Dervan, P. B. (2000) Activation of gene expression by small molecule transcription factors, *Proc. Natl. Acad. Sci. U.S.A. 18*, 4359−4363.
19. Chiang, S. Y., Burli, R. W., Benz, C. C., Gawron, L., Scott, G. K., Dervan, P. B., and Beerman, T. A. (2000) Targeting the ets-1 binding site of the her2/neu promoter with pyrrole-imidazole polyamides, *J. Biol. Chem. 275*, 24246−24254.
20. Gearhart, M. D., Dickinson, L., Ehley, J., Melander, C., Dervan, P. B., Wright, P. E., and Gottesfeld, J. M. (2005) Inhibition of DNA binding by human estrogen-related receptor 2 and estrogen receptor α with minor groove binding polyamides, *Biochemistry 44*, 4196−4203.
21. Lai, Y-M., Fukada, N., Ueno, T., Matsuda, H., Saito, S., Matsumoto, K., Ayame, H., Bando, T., Sugiyama, H., Mugishima, H., and Serie. K. (2005) Synthetic pyrrole-imidazole polyamide inhibits expression of the human transforming growth factor-β1 gene, *J. Pharm. Exp. Ther. 315*, 571−575.
22. Matsuda, H., Fukuda, N., Ueno, T., Tahira, Y., Ayame, H., Zhang, W., Bando, T., Sugiyama, H., Saito, S., Matsumoto, K., Mugishima, H., and Serie. K. (2006) Development of gene silencing pyrrole-imidazole polyamide targeting the TGF-β1 promoter for the treatment of progressive renal diseases, *J. Am. Soc. Nephrol. 17*, 422−432.
23. Burnett, R., Melander, C., Puckett, J. W., Son, L. S., Wells, R. D., Dervan, P. B., and Gottesfeld, J. M. (2006) DNA sequence-specific polyamides alleviate transcription inhibition associated with long GAA. TTC repeats in Friedreich's ataxia, *Proc. Natl. Acad. Sci. U.S.A. 103*, 11497−11502.
24. Le, N. M., Sielaff, A. M., Cooper, A. J., Mackay, H., Brown, T., Kotecha, M., O'Hare, C., Hochhauser, D., Lee, M., and Hartley, J. A. (2006) Binding of f-PIP, a pyrrole- and imidazole-containing triamide, to the inverted CCAAT box-2 of topoisomerase II alpha promoter and modulation of gene expression in cells, *Bioorg. Med. Chem. Lett. 16*, 6161−6164.
25. Hochhauser, D., Kotecha, M., O'Hare, C., Morris, P. J., Hartley, J. M., Taherbhai, Z., Harris, D., Forni, C., Mantovani, R., Lee, M., and Hartley, J. A. (2007) Modulation of topoisomerase IIα expression by a DNA sequence-specific polyamide, *Mol. Cancer Ther. 6*, 346−354.
26. Buchmueller, K. L., Staples, C. M., Howard, C. M., Horick, S. M., Uthe, P. B., Le, M., Cox, K. K., Nguyen, B., Pacheco, K. A. O., Wilson, W. D., and Lee, M. (2005) Extending the language of DNA molecular recognition by polyamides: unexpected influence of imidazole and pyrrole arrangement on binding affinity and specificity, *J. Am. Chem. Soc. 127*, 742−750.
27. Buchmueller, K. L., Staples, A. M., Uthe, P. B., Howard, C. M., Pacheco, K. A. O., Cox, K. K., Henry, J. A., Bailey, S. L., Horick, S. M., Nguyen, B., Wilson, W. D., and Lee, M. (2005) Molecular recognition of DNA base pairs by the formamido/pyrrole and formamido/imidazole pairings in stacked polyamides, *Nucleic Acids Res. 33*, 912−921.
28. Kumar, S., Bathini, Y., Joseph, T., Pon, R., and Lown, J. W. (1991) Structural and dynamic aspects of non-intercalative (1:1) binding of a thiazole-lexitropsin to the decadeoxyribonucleotide d-[CG-CAATTGCG]$_2$: an ^{1}H-NMR and molecular modelling study, *J. Biomol. Struct. Dyn. 9*, 1−21.
29. Chen, Y-H., Yang, Y., and Lown, J. W. (1996) Optimisation of cross-linked lexitropsins, *J. Biomol. Struct. Dyn. 14*, 341−355.
30. Mrksich, M., Parks. M. E., and Dervan, P. B. (1994) Hairpin peptide motif; a new class of oligopeptides for sequence specific recognition in the minor groove of double helical DNA, *J. Am. Chem. Soc. 116*, 7983−7988.
31. Mrksich, M., and Dervan, P. B. (1993) Enhanced sequence specific recognition in the minor groove of DNA by covalent peptide dimers: bis(pyridine-2-carboxamideonetropsin)$(CH_2)_{3-6}$, *J. Am. Chem. Soc. 115*, 9892−9899.
32. Mrksich, M., and Dervan, P. B. (1994) Design of a covalent peptide heterodimer for sequence-specific recognition in the minor groove of double helical DNA, *J. Am. Chem. Soc. 116*, 3663−3664.
33. Chen, Y-H., and Lown, J. W. (1994) A new DNA minor groove binding motif: cross-linked lexitropsins, *J. Am. Chem. Soc. 116*, 6995−7005.
34. Dervan, P. B., and Burli, R. W. (1999) Sequence-specific recognition by polyamides, *Curr. Opin. Chem. Biol. 3*, 688−693.
35. Chen, Y-H., and Lown, J. W. (1995) Design and synthesis of sequence specific DNA minor groove recognising ligands of the cross-linked lexitropsin class, *Heterocycles 41*, 1691−1707.
36. Chen, Y-H., and Lown, J. W. (1995) DNA minor groove binding of cross-linked lexitropsins: expermiental conditions required to observe the covalently linked WPPW (groove wall-peptide-peptide groove wall) motif, *Biophys. J. 68*, 2041−2048.
37. O'Hare, C. C., Mack, D., Tandon, M., Sharma, S. K., Lown, J. W., Kopka, M. L., Dickerson, R. E., and Hartley, J. A. (2002) DNA sequence recognition in the minor groove by crosslinked polyamides: the effect of N-terminal head group and linker length in binding affinity and specificity, *Proc. Natl. Acad. Sci. U.S.A. 99*, 72−77.
38. Lacy, E. R., Le, N. M., Price, C. A., Lee, M., and Wilson, W. D. (2002) Influence of a terminal formamido group on the sequence recognition of DNA by polyamides, *J. Am. Chem. Soc. 124*, 2153−2163.
39. Buchmueller, K. L., Bailey, S. L., Matthews, D. A., Taherbhai, Z. T., Register, J. K., Davis, Z. S., Bruice, C. D., O'Hare, C. C., Hartley, J. A., and Lee, M. (2006) Physical and structural basis for the strong interactions of the −ImPy− central pairing motif in the polyamide f-ImPyIm, *Biochemistry 45*, 13551−13565.
40. Biacore. (1997) *BIAevaluation version 3.0: Software Handbook*, Biacore AB, Uppsala, Sweden.
41. Lyng, R., Rodger, A., and Norden, B. (1991) The CD of ligand-DNA systems. 1. poly (dG-dC) B-DNA, *Biopolymers 31*, 1709−1720.
42. Lyng, R., Rodger, A., and Norden, B. (1992) The CD of ligand-DNA systems. 2. poly (dA-dT) B-DNA, *Biopolymers 32*, 1201−1214.
43. Buchmueller, K. L., Taherbhai, Z., Howard, C. M., Bailey, S. L., Nguyen, B., O'Hare, C., Hochhauser, D., Hartley, J. A., Wilson, W. D., and Lee, M. (2005) Design of a hairpin polyamide, ZT65B, for targeting the inverted CCAAT box (ICB) site in the multidrug resistant (MDR1) gene, *ChemBioChem 6*, 2305−2311.
44. Myszka, D. G., He, X., Dembo, M., Morton, T. A., and Goldstein, B. (1998) Extending the range of rate constants available from BIACORE: interpreting mass transport-influenced binding data, *Biophys. J. 75*, 583−594.
45. Karlsson, R. (1999) Affinity analysis of non-steady-state data obtained under mass transport limited conditions using BIACORE technology, *J. Mol. Recognit. 12*, 285−292.
46. Nguyen, B., Tanious, F. A., and Wilson, W. D. (2007) Biosensor-Surface Plasmon Resonance: Quantitative Analysis Of Small Molecule-Nucleic Acid Interactions, *Methods 42*, 150−161.
47. Myszka, D. G. (2000) Kinetic, equilibrium and thermodynamic analysis of macromolecular interactions with BIACORE, *Methods Enzymol. 323*, 325−340.
48. White, S., Szewczyk, Turner, J. W., Baird, E. E., and Dervan, P. B. (1998) Recognition of the four Watson-Crick base pairs in the DNA minor groove by synthetic ligands, *Nature 391*, 468−471.

49. Renneberg, D., and Dervan, P. B. (2003) Imidazopyridine/pyrrole and hydroxy-benimidazole/pyrrole pairs for DNA minor groove recognition, *J. Am. Chem. Soc. 125*, 5707−5716.
50. Wellenzohn, B., Loferer, M. J., Trieb, M., Rauch, C., Winger, R. H., Mayer, E., and Liedl, K. R. (2003) Hydration of hydroxypyrrole influences binding of ImHpPyPy-beta-Dp polyamide to DNA, *J. Am. Chem. Soc. 125*, 1088−1095.
51. Marques, M. A., Doss, R. M., Foister, S., and Dervan, P. B. (2004) Expanding the repertoire of heterocycle ring pairs for programmable minor groove DNA recognition, *J. Am. Chem. Soc. 126*, 10339−10349.
52. Baliga, R., Baird, E. E., Herman, D. M., Melander, C., Dervan, P. B., and Crothers, D. M. (2001) Kinetic consequences of covalent linkage of DNA binding polyamides, *Biochemistry 40*, 3−8.

BI701053A